



CHORUS

This is the accepted manuscript made available via CHORUS. The article has been published as:

Cubic H₃S around 200 GPa: An atomic hydrogen superconductor stabilized by sulfur

D. A. Papaconstantopoulos, B. M. Klein, M. J. Mehl, and W. E. Pickett

Phys. Rev. B **91**, 184511 — Published 19 May 2015

DOI: [10.1103/PhysRevB.91.184511](https://doi.org/10.1103/PhysRevB.91.184511)

Cubic H₃S around 200 GPa: an atomic hydrogen superconductor stabilized by sulfur

D. A. Papaconstantopoulos¹, B. M. Klein², M. J. Mehl³, and W. E. Pickett^{2*}

¹Computational Materials Science Center, George Mason University, Fairfax, VA USA

²Department of Physics, University of California Davis, Davis, CA 95616, USA

³Center for Computational Materials Science, Naval Research Laboratory, Washington DC 20375, USA

The multiple scattering-based theory of Gaspari and Gyorffy for the electron-ion matrix element in close packed metals is applied to $Im\bar{3}m$ H₃S, which has been predicted by Duan *et al.* and Bernstein *et al.* to be the stable phase at this stoichiometry around 190 GPa, thus is the leading candidate to be the phase observed to superconduct at 190K by Drozdov, Erements, and Troyan. The nearly perfect separation of vibrational modes into those of S and of H character provides a simplification that enables identification of contributions of the two atoms separately. The picture that arises is basically that of superconducting atomic H stabilized by strong covalent mixing with S p and d character. The reported isotope shift is much larger than the theoretical one, suggesting there is large anharmonicity in the H vibrations. Given the relative unimportance of sulfur, hydrides of lighter atoms at similarly high pressures may also lead to high temperature superconductivity.

I. BACKGROUND

The report by Drozdov, Erements, and Troyan¹ (DET) of superconductivity up to $T_c=190$ K in H₂S compressed to the 200 GPa regime has reignited excitement in the possibility of achieving room temperature superconductivity. This report builds on previous success of pressure enhancement of T_c in a variety of types of materials: from 134K to 164K in the cuprate Hg2223,^{2,3} from zero to 20-25 K in the simple metals Li, Ca, and Y,[4-10] and from zero to 14K in the insulator silicon.¹¹ An anticipated major factor is the increase in the phonon energy scale with compression, since it sets the temperature scale for T_c , as pointed out early on¹² and reviewed more recently¹³ by Ashcroft in predicting possible room temperature superconductivity in metallic hydrogen.

The newly reported high values of T_c appear to confirm theoretical predictions that predated the experiment. Applying particle swarm crystal structure search techniques founded on density functional theory, Li *et al.* predicted¹⁴ candidate stable crystal structures of H₂S up to 220 GPa. These predictions were followed by linear response calculations of the phonon spectrum ω_Q , electron-phonon matrix elements, and finally the Eliashberg spectral function $\alpha^2F(\omega)$, from which T_c can be calculated, depending only mildly on the presumed value of the retarded Coulomb repulsion $\mu^* = 0.10-0.13$. For pressures of 140-180 GPa, they obtained an electron-phonon coupling strength $\lambda=1.0-1.2$, an Allen-Dynes characteristic frequency¹⁵ $\omega_{log}\sim 1000$ K, and T_c of 40K at 140 GPa and peaking at 80 K at 160 GPa. While 80K is well short of the reported $T_c=190$ K, the result is convincing that very high T_c is predicted in H₂S at high pressure.

The sister stoichiometry H₃S has been explored in very similar fashion by Duan *et al.*¹⁶ Predicting structures to more than 200 GPa, their linear response results for $Im\bar{3}m$ H₃S led to very large calculated values of electron-phonon coupling strength $\lambda=2.0-2.2$, frequency scales $\omega_{log}\sim 1300$ K, and values of T_c up to 200K. In the calculations of Li *et al.* and Duan *et al.*, the high values

of ω_{log} are expected from the anticipated increase of force constants as volume is decreased. The large values of λ , a factor of two or more over most other very good superconductors (including MgB₂), imply that the electronic matrix elements are substantially larger than in nearly all known conventional superconductors.

In this report we use Gaspari-Gyorffy (GG) theory¹⁷ to provide insight into why electron-ion matrix elements vary, and evidently increase strongly, with pressure. Such understanding is necessary not only to interpret the results described above, but also to provide essential clues how to increase matrix elements, and λ , at lower or possibly ambient pressure. Interestingly, shortly after the formulation of this theory, two of the present authors applied it to predict $T_c\sim 250$ K in metallic hydrogen at a few Mbar pressure.¹⁸

GG theory¹⁷ builds on the earlier observation of Hopfield¹⁹ that electron scattering off (moving) ions has strong local character. First, metallic screening means the Thomas-Fermi screening length is short, of the order of 1 Å, and very weakly dependent on carrier density (more correctly, the Fermi level density of states [DOS] $N(E_F)$). GG employed a multiple scattering Green's function formalism that facilitated three simplifications. The first is that the potential is spherical (very good approximation) and is negligible beyond the atomic sphere; the second is that the linear change in potential of a displaced ion can be approximated by a rigid shift of the atomic potential. Thirdly, the direction dependence of the wavefunction coefficients is averaged out, thereby neglecting any special influence of Fermi surface shape. The H₃S Fermi surface²⁰ is large and multisheeted, minimizing the likelihood of Fermi surface effects. It is possible that these approximations may improve with reduction in volume, in any case these approximations should not degrade as the system become denser. The bands shown by Duan *et al.*¹⁶ and Bernstein *et al.*²⁰ for the $Im\bar{3}m$ structure of H₃S that we discuss show much free electron, spherical character in the lower 75% of the occupied bands, though less so around the Fermi energy where S $3p$ - H $1s$ hybridization produces structure in the DOS.

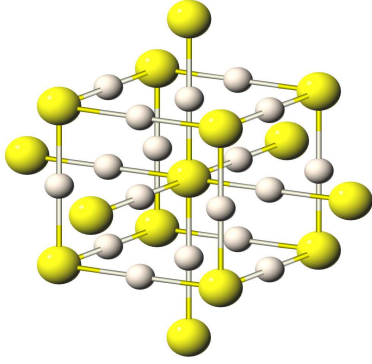


FIG. 1: (Color online) The $Im\bar{3}m$ crystal structure of H_3S , illustrating the two interlaced ReO_3 sublattices. Large sphere is S, small sphere is H.

II. THEORY AND RESULTS

The coupling strength λ , and the frequency weighting spectrum $g(\omega)$ normalized to unity, are given in Eliashberg theory²¹ by

$$\lambda = 2 \int \frac{\alpha^2 F(\omega)}{\omega} d\omega; \quad g(\omega) = \frac{2\alpha^2 F(\omega)}{\lambda\omega}, \quad (1)$$

where $\alpha^2 F$ is the Eliashberg electron-phonon spectral function that governs many superconducting properties. The calculations by Li *et al.* for H_2S and Duan *et al.* for H_3S demonstrate that the lower range of phonon frequencies (the acoustic modes) have negligible H character, while the optic modes above the gap at 20-25 THz have negligible S character, making it an ideal platform for applying the GG expression to the atoms *separately*.

Thus $\lambda = 3\lambda_H + \lambda_S$, where the latter arise from the integral over the low frequency S modes, the former from the nine higher frequency H branches. In this case the GG expression, given originally for an elemental solid, can be applied to the S and H spheres separately.²² Each atomic (j) coupling constant λ_j is given by the integral over the appropriate frequency region, leading to

$$\lambda_j = \frac{N(E_F) \langle I_j^2 \rangle}{M_j \omega_j^2} \equiv \frac{\eta_j}{M_j \omega_j^2}. \quad (2)$$

The averaged matrix elements $\langle I^2 \rangle$ obtained from GG theory are discussed below.

The separation of mode character also allows a simple estimate of the total frequency moments that enter the Allen-Dynes (AD) equation for T_c , through the weight function

$$g(\omega) = [\lambda_S g_S(\omega) + 3\lambda_H g_H(\omega)] / (\lambda_S + 3\lambda_H), \quad (3)$$

where the partial g_j functions, defined analogously to that of AD (Eq. 1) are separately normalized to unity.

Both H_2S and H_3S having been shown^{14,16} to have strong electron-phonon coupling at high pressure. Bernstein *et al.*²⁰ have provided convincing evidence that H_2S

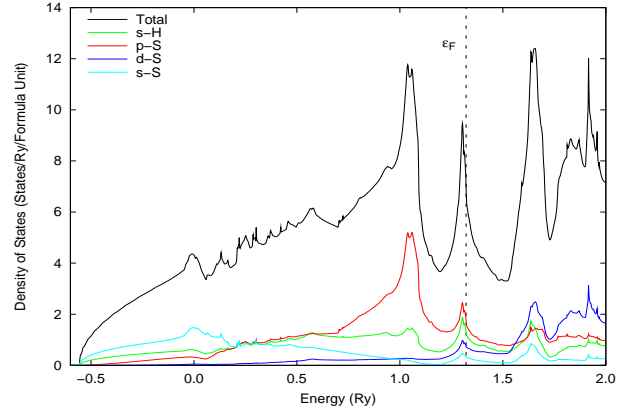


FIG. 2: (Color online) Total and orbital-projected densities of states of H_3S at 210 GPa ($a=5.6$ a.u.). Note the position of E_F within the sharp and narrow peak, and that the H 1s contribution is that from all three H atoms.

is unstable to decomposition into bcc H_3S and sulfur, and that competing stoichiometries are unlikely. This result confirms the suggestion of DET, who reported sulfur formation in their samples. Because of this evidence on the most likely superconducting phase, we focus on $Im\bar{3}m$ H_3S with its simple *bcc* structure based in two interlaced ReO_3 structure sublattices. From $\alpha^2 F$ of Duan *et al.*, we simplify with a constant $\alpha^2 F_j$ (constant for each atom species j) with frequency ranges (in kelvin) of [430,820] for S and [1250,2500] for H. Results are insensitive to these limits, depending mostly on the mean frequencies and the separation of λ into S and H contributions. The resulting frequency moments ω_{log} , ω_1 , and ω_2 and associated data, for insight into separate S and H contribution, for use in the AD equation,¹⁵ and to compare with results below from GG theory, are presented in Table I.

With $\mu^*=0.15$, $T_c=234$ K results; the difference from the value quoted by Duan *et al.* might be due to neglect of the strong coupling factor $f_1=1.13$ factor in the AD equation, which amounts to a 26 K increase, or partially to our constant $\alpha^2 F$ modeling. Neglecting the contribution from the S modes, λ is decreased from 2.2 to 1.5 but ω_{log} increases from 1500 K to 1770 K, and T_c decreases by only 19 K to 215 K. The sulfur contribution to T_c is 8%; H_3S is basically an atomic hydrogen high temperature superconductor. Bernstein *et al.* also suggested that S vibrations are not essential for the high T_c . The H isotope effect can also be obtained. λ is unaffected by masses; $M\omega^2$ is a function of the force constants alone, so frequencies, specifically ω_{log}^H decrease as the square root of the mass. The resulting critical temperature is reduced to ~ 170 K, slightly more than $234 \text{ K}/\sqrt{2}$ because the small S contribution remains unchanged. The experimental value of DET¹ is 90 K; the most likely cause of this discrepancy is strong anharmonicity of the H optic modes.

The second moment frequency at 200 GPa of S is $\omega_2^S=615$ K, while that of H is $\omega_2^H=1840$ K, thus with the

atomic masses of 32 and 1 a.m.u respectively, the denominator $M\omega_2^2$ is $32/9=3.5$ larger for S. The consequence is that a given contribution to η_H is $3.5\times 3\sim 10$ times more effective in increasing λ than the same contribution to η_S (though in practice there is no clear method of effecting such a tradeoff).

TABLE I: Electron-phonon coupling data for H_3S , obtained from modeling the results of Duan *et al.* with a constant α^2F model. Frequencies are in Kelvin.

	S	H	Total
ω_{log}	595	1770	1500
ω_1	605	1800	1530
ω_2	615	1840	1560
$M\omega_2^2$ (eV/Å ²)	9.3	2.6	–
η (eV/Å ²)	4.7	1.48	–
λ	0.5	1.7/3	2.2

In terms of the phase shifts $\delta_{\ell,j}$ for the j -th atom for orbital channel ℓ , the square electron-ion matrix element averaged of the Fermi surface can be written in the simple form¹⁷ as

$$\langle I_j^2 \rangle = \frac{E_F}{\pi^2} \frac{1}{N(E_F)^2} \sum_{\ell=0}^2 2(\ell+1) \sin^2(\delta_\ell - \delta_{\ell+1}) \nu_\ell \nu_{\ell+1}, \quad (4)$$

where $\nu_\ell = N_\ell(E_F)/N_\ell^{(1)}$ is the ratio of the ℓ -th partial DOS to $N^{(1)}$, the single scatterer DOS, for the given atomic potential in a homogeneous system. $\langle I^2 \rangle$ is independent of $N(E_F)$ since it can equally well be expressed²³ in terms of the fractions $N_\ell(E_F)/N(E_F)$ which usually do not reflect the van Hove singularities of either one. The calculated DOS at 210 GPa is shown in Fig. 2. The Fermi level falls at the peak of a sharp and narrow peak; calculations at other volumes indicate this is a persistent occurrence. $\langle I_j^2 \rangle$ will tend to be maximized in the cases where “neighboring” channels $\ell, \ell+1$ have a large difference in phase shifts but as similar as possible ratios ν_ℓ . From the GG expression, for each atom $\eta_j = N(E_F)\langle I_j^2 \rangle$, and the latter factor involves the $\sin^2(\delta_\ell - \delta_{\ell+1})$ factor and products of PDOS ratios $\nu_\ell \nu_{\ell+1}$. $M_j \omega_j^2$ can be expressed in terms of the ionic force constants, independent of M_j , (which we return to below) so that any isotope effect different from $M^{-1/2}$ will arise from factors beyond λ (primarily anharmonicity).

The calculations have been carried out with two all-electron linearized augmented plane wave (LAPW) codes, one developed at NRL,²⁴ and also ELK.²⁵ The sphere radii were 1.8 a.u. and 1.0 a.u. for S and H respectively, except for the smallest volume where the S radius was reduced because the sum of the radii must be no more than $a/2$.

The band structure^{16,20} consists of four nearly filled bands, leaving some holes at Γ and electrons around N. In addition, a fifth broad band is roughly half filled. The DOS is noteworthy: free electron like over 20 eV of the valence band before strong structure arises in a ± 7

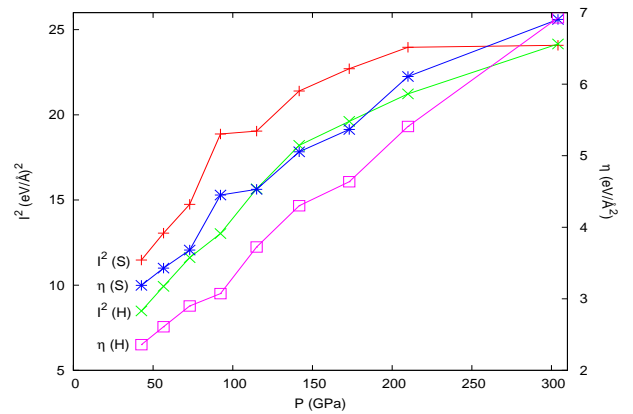


FIG. 3: (Color online) Plots demonstrating the very strong pressure increase of $\langle I^2(j) \rangle$ (left axis) and η_j (right axis) for $j=S$ and H in $Im\bar{3}m$ H_3S . For H, the η plotted is the total for 3 H atoms.

eV range centered at E_F , which lies very close (slightly above) the strong and sharp peak in the DOS. This peak at E_F persists for all pressures from $P=0$ to 300 GPa and even above, almost as if E_F were pinned at this peak, while other features of the DOS evolve.

Table II shows the Fermi level values of total and angular momentum components of the electronic densities of states across a wide range of volumes. Even though $Im\bar{3}m$ H_3S may not be stable at lower pressures, we provide results for the large range $P=0-210$ GPa to observe the effect of interatomic distance on the electronic structure and coupling. While the total $N(E_F)$ shows a weak non-monotonic variation, the ℓ -components have a stronger lattice constant (pressure) dependence. As expected the sulfur $3p$ -like states are the dominant component but a strong participation of $3d$ character especially at high pressures is present, hybridizing with the also strong and nearly constant H $1s$ contribution.

Now we discuss the electronic factor η_j . It should be kept in mind that the relative importance for T_c of H versus S modes is not simply λ_j , but more like $\lambda_j \omega_{2,j}$ which is a factor of ten greater for 3H than for S). For hydrogen, which dominates the contribution to T_c only the $s-p$ channel is relevant at all pressures. The phase shift factor $\sin^2(\delta_s - \delta_p)$ decreases with pressure. Fig. 3 illustrates the factor of two increase in η_H from $P=100$ GPa to 300 GPa. This dramatic increase results from an even larger increase in the PDOS product $\nu_s^H \nu_p^H$, reflecting transfer of $1s$ character to $2p$ character. In the spherical harmonic expansion of the atomic wavefunctions this ‘ $2p$ ’ character represent the expansion of tails of the orbitals on neighboring atoms that gives rise to the increased H-S hybridization under pressure.

As noted above from our analysis of the results of Duan *et al.*, the sulfur contribution is less important. As for H, the increase in η occurs in spite of a decrease in the $\sin^2(\delta_p - \delta_d)$ factor, by 30% from $P=100$ to $P=300$ GPa. Over this pressure range, the PDOS ratio product $\nu_p^S \nu_d^S$

TABLE II: Total and angular-momentum decomposed densities of electronic states at the Fermi level (states/Ry/both spins) in $Im\bar{3}m$ H₃S. The ℓ -components are projections within sphere radii R(S)=1.8 a.u. and R(H)=1.0 a.u.

a (a.u.)	N(E_F)	S-s	S-p	S-d	H-s/atom
5.6	6.93	0.325	1.74	0.751	0.435
5.8	6.43	0.286	1.53	0.605	0.405
6.0	6.47	0.274	1.46	0.528	0.415
6.2	6.42	0.253	1.18	0.528	0.462
6.4	6.79	0.259	1.36	0.417	0.455
6.6	7.15	0.255	1.38	0.375	0.482
6.8	7.56	0.254	1.42	0.339	0.513

increases by 75%, giving a net η increase by more than 50%. In addition, the S s - p and even d - f channels begin to contribute, reaching 20% of the total of $\langle I^2 \rangle$ at 300 GPa. Thus the increase is a composite effect of increase of both d and s character of S, which is reflected also in the growing phase shifts of these channels. These transfers of atomic character under pressure are consistent with general expectations of the evolution of atomic character under reduction of volume. Interpolating to 200 GPa to obtain $\eta_S=5.84$ eV/Å², $\eta_H=1.71$ eV/Å² (which must be multiplied by three), and using the frequency moments from Table 1, we obtain $\lambda=2.6$, thus $T_c \sim 250K$ depending somewhat on the chosen value of $\mu^*=0.10$ - 0.13 . This value is very consistent with the value of T_c (above) obtained from our modeling of the Duan data. Though the numbers might vary for other low-Z hydrides (H_nP, H_nB, ...) the lack of any special role of S in these results suggests there should also be a strong increase in T_c with pressure in other low-Z element hydrides.

A question of great interest is whether T_c increases further at higher pressure. The data presented in Table III provides the pressure dependence of the important quantities entering η_S and η_H . This data demonstrates that the strongest contributions arise for sulfur from the pd channel and for hydrogen from the sp channel. Note that for H one should multiply by three to account for the three H atoms in the unit cell.

Since λ_H dominates the sulfur contribution, we can focus on the H contribution alone. The total pressure derivative contains several contributions

$$\begin{aligned} \frac{d \log T_c}{dP} &= \frac{d \log \omega_{log}}{dP} + \frac{d \log f_1}{dP} + \frac{d \log E(\lambda)}{dP} \\ &= \frac{d \log \omega_{log}}{dP} + \left(\frac{d \log f_1}{d\lambda} + \frac{d \log E(\lambda)}{d\lambda} \right) \frac{d\lambda}{dP}, \end{aligned} \quad (5)$$

where f_1 is the strong coupling correction and $E(\lambda)$ is the exponential term in the Allen-Dynes equation. The pressure variation of the $M\omega_H^2$ denominator is challenging to approximate without full calculations of the spectrum and α^2F . We have modeled the variation of the H spectrum by assuming the three 3-fold Γ point optic modes are representative. The lower two of these modes are IR-active involving H-S bond stretch and bond bend-

ing modes, the hardest frequency is a silent mode with quadrupolar H motion with respect to S.

From calculations of these Γ frequencies in the 240-270 GPa range using the ELK code we calculate a positive but modest pressure increase $d \log \bar{\omega}_H / dP \approx 1.9 \times 10^{-3}$ GPa⁻¹. From Fig. 3 we obtain $d \log \eta_H / dP = 3.5 \times 10^{-3}$ GPa⁻¹, thus λ decreases with pressure approximately as $d \log \lambda_H / dP \sim -0.3 \times 10^{-3} / \text{GPa}$. However, to our precision this is indistinguishable from zero, so the pressure derivative in Eq. 5 reduces to the first term, the frequency derivative. The resulting prediction is a small increase $dT_c/dP = 0.4$ K/GPa. This result disagrees in sign with Duan *et al.*, who quoted a smaller (in magnitude) negative value of $dT_c/dP = -0.12$ K/GPa from direct calculation, however both numbers are small compared to the large value of T_c itself, so there is no significant disagreement.

III. CONCLUSIONS

The report by DET of T_c up to 190 K in H_nS samples has breathed new life into the 50 year old expectation of high T_c in atomic H systems. Both Li *et al.* and Duan *et al.* had found that Eliashberg theory and linear response results for electron-phonon coupling account for T_c in the 80-200 K range for H₂S and H₃S at high pressure, and the analysis of Bernstein *et al* make $Im\bar{3}m$ H₃S the primary candidate to be this record-high temperature superconductor. In this paper we have established that the coupling of H vibrations increases strongly for pressures up to and even beyond 210 GPa, and that 90+% of the coupling arises from H vibrations in this hydride that is stabilized by hybridization²⁰ with S. This picture is analogous to the finding of the essential contribution of H in the superconductor PdH at ambient pressure,²⁶ and the broader picture of Ashcroft¹² of superconducting elemental H at high pressure. The theoretical isotope shift of T_c based on the harmonic approximation is not in agreement with the experimental result, suggesting substantial H anharmonicity will be necessary to understand before the picture is complete. Our picture, which relies on coupling across the large Fermi surface, is at odds with the hole superconductivity picture of Hirsch and Marsiglio.²⁷

Acknowledgments.

The authors acknowledge many insightful conversations on the theory and application of GG theory with the late B. L. Györfy, to whom we dedicate this paper. We acknowledge discussions with A. S. Botana, F. Gygi, and I. I. Mazin. M.J.M. was supported by the U.S. Office of Naval Research through the Naval Research Laboratory's basic research program. W.E.P. was supported by NSF award DMR-1207622-0. D.A.P. was supported by grant N00173-11-1-G002 from the U.S. Naval Research Laboratory.

TABLE III: Pressure variation of the Hopfield parameter η (eV/Å²) and electron-ion squared matrix element $\langle I^2 \rangle$ (eV²/Å²), both decomposed into the three channels sp , pd , and df for S, and the H sp channel (given for a single atom).

a (a.u.)	P (GPa)	S η_{sp}	S I_{sp}^2	S η_{pd}	S I_{pd}^2	S η_{df}	S I_{df}^2	H η_{sp}	H I_{sp}^2
5.6	210	0.68	2.66	5.12	20.1	0.31	1.21	1.80	7.06
5.8	142	0.39	1.65	4.45	18.9	0.21	0.89	1.43	6.06
6.0	92	0.24	1.00	4.14	17.4	0.15	0.63	1.24	5.21
6.2	57	0.19	0.78	4.13	17.5	0.13	0.57	1.02	4.34
6.4	31	0.08	0.33	3.52	14.1	0.08	0.31	0.96	3.87
6.6	13	0.05	0.18	3.37	12.7	0.06	0.21	0.87	3.31
6.8	0	0.02	0.09	3.12	11.2	0.04	0.14	0.79	2.83

- * Electronic address: pickett@physics.ucdavis.edu
- ¹ A. P. Drozdov, M. I. Erements, and I. A. Troyan, arXiv:1412.0460.
 - ² A. Schilling, M. Cantoni, J. D. Guo, and H. R. Ott, Nature **363**, 6424 (1993).
 - ³ C. W. Chu, L. Gao, F. Chen, Z. J. Huang, R. L. Meng, and Y. Y. Xue, Nature **365**, 323 (1993).
 - ⁴ References to the experimental literature are given by J. S. Schilling, Physica C **460-462**, 182 (2007) and M. Debessai, J. J. Hamlin, and J. S. Schilling, Phys. Rev. B **78**, 064519 (2008).
 - ⁵ D. Kasinathan, J. Kuneš, A. Lazicki, H. Rosner, C. S. Yoo, R. T. Scalettar, and W. E. Pickett, Phys. Rev. Lett. **96**, 047004 (2006).
 - ⁶ D. Kasinathan, K. Koepernik, J. Kunes, H. Rosner, and W. E. Pickett, Physica C **460-462**, 133-6 (2007).
 - ⁷ L. Shi and D. A. Papaconstantopoulos, Phys. Rev. B **73**, 184516 (2006).
 - ⁸ Z. P. Yin, F. Gygi, and W. E. Pickett, Phys. Rev. B **80**, 184515 (2009).
 - ⁹ Z. P. Yin, S. Y. Savrasov, and W. E. Pickett, Phys. Rev. B **74**, 094519 (2006).
 - ¹⁰ S. Lei, D. A. Papaconstantopoulos, and M. J. Mehl, Phys. Rev. B **75**, 024512 (2007).
 - ¹¹ N. Buckel and J. Wittig, Phys. Lett. **17**, 187 (1965).
 - ¹² N. W. Ashcroft, Phys. Rev. Lett. **21**, 1748 (1968).
 - ¹³ N. W. Ashcroft, Phys. Rev. Lett. **92**, 187002 (2004).
 - ¹⁴ Y. Li *et al.*, J. Chem. Phys. **140**, 174712 (2014).
 - ¹⁵ P. B. Allen and R. C. Dynes, Phys. Rev. B **12**, 905 (1975).
 - ¹⁶ D. Duan *et al.*, Sci. Rep. **4**, 6968 (2014).
 - ¹⁷ G. D. Gaspari and B. L. Györfy, Phys. Rev. Lett. **28**, 801 (1972).
 - ¹⁸ D. A. Papaconstantopoulos and B. M. Klein, Ferroelectrics **16**, 307 (1977); D. A. Papaconstantopoulos *et al.*, Phys. Rev. B **15** 4221 (1977).
 - ¹⁹ J. J. Hopfield, Phys. Rev. **186**, 443 (1969).
 - ²⁰ N. Bernstein, C. S. Hellberg, M. D. Johannes, I. I. Mazin, and M. J. Mehl, Phys. Rev. B **91**, 060511(R) (2015).
 - ²¹ D. J. Scalapino, J. R. Schrieffer, and J. W. Wilkins, Phys. Rev. **148**, 263 (1966).
 - ²² B. M. Klein and D. A. Papaconstantopoulos, J. Phys. F: Metal Phys. **6**, 1135 (1976).
 - ²³ W. E. Pickett, Physica B+C **111B**, 1 (1981).
 - ²⁴ The NRL LAPW code, originally developed by H. Krakauer and D. J. Singh, was used with Hedin-Lundqvist exchange-correlation. DOS results were generated from 285 k points in the irreducible Brillouin zone with the tetrahedron method. Total energies were fit to the Birch equation to obtain the P(V) equation of state.
 - ²⁵ <http://elk.sourceforge.net>
 - ²⁶ D. A. Papaconstantopoulos and B. M. Klein, Phys. Rev. Lett. **35**, 110 (1975); B. M. Klein *et al.*, Phys. Rev. Lett. **39**, 574 (1977); D. A. Papaconstantopoulos, B. M. Klein, E. N. Economou and L. L. Boyer Phys. Rev. B **17**, 141 (1978).
 - ²⁷ J. E. Hirsch and F. Marsiglio, arXiv:1412.6251.